



OPEN Ocular blood flow in preterm neonates

Ronald H. Silverman^{1,2✉}, Raksha Urs¹, Jason D. Horowitz¹, Osode Coki¹ & Leora Pinto¹

Retinopathy of prematurity (ROP) is a disorder affecting low birthweight, preterm neonates. In the preterm eye, the retina is not fully developed and neovascularization may occur at the margin between the developed vascular retina and undeveloped avascular retina. Without timely treatment by laser or intravitreal anti-vascular endothelial growth factor (VEGF) therapy, this can lead to tractional retinal detachment and blindness. Visualization of the retina in regular examinations by indirect ophthalmoscopy is hence the current standard of care, but the exams are stressful and interpretation of images is subjective. The upregulation of VEGF in ROP would suggest an increase in ocular blood flow. In this report, we evaluate the potential of ultrafast plane-wave Doppler ultrasound (PWU) to detect increased flow velocities in the orbital vessels supplying the eye in a gentle exam with objective findings. We imaged both eyes of 50 low-birthweight preterm neonates using 18 MHz PWU. Flow velocity in the central retinal artery (CRA) and vein (CRV), and the short posterior ciliary arteries were determined and values at each ROP Stage compared. We found significantly increased velocities in the CRA and CRV in Stage 3 ROP eyes, where intervention would be considered. We compared multivariate models for identifying Stage 3 eyes comprised solely of clinical factors, solely of Doppler parameters, and clinical plus Doppler parameters. The respective models provided areas under their respective ROC curves of 0.760, 0.812, and 0.904. PWU Doppler represents a gentle, objective means for identifying neonates at risk for ROP that could complement ophthalmoscopy.

Retinopathy of prematurity (ROP) is a potentially devastating disorder of retinal vascular development occurring in low birthweight, preterm neonates. In spite of advances in neonatal intensive care, ROP remains a leading cause of pediatric blindness and potential lifelong visual impairment¹. ROP incidence among premature infants in the United States has increased, especially among the Black and Hispanic populations².

Starting at about 16 weeks gestation, the retina develops from the optic nerve outwards, a process that is complete at about 40 weeks³. The retinal vasculature is thus incompletely developed and immature in preterm neonates.

Oxygen plays a central role in retinal vessel development^{4,5}. In utero, 'physiological hypoxia' allows normal retinal angiogenesis, primarily at the retinal periphery^{5,7}, with VEGF playing a key role⁸. After preterm delivery and exposure to higher oxygen levels, there is cessation of vessel development and loss of already formed vessels. The avascular retina becomes more metabolically active and VEGF is upregulated; pathologic neovascularization with the potential for retinal detachment then follows⁷.

The current standard of care for preterm neonates entails examination of the eye by indirect ophthalmoscopy or wide-angle contact photography (RetCam, Natus Medical, Pleasanton, CA) on a regular basis. The first eye screening exam is appropriate at 4 weeks of age for neonates with gestational age (GA) of 27 weeks or more and at up to 9 weeks for progressively lower GA. Follow-up exams may occur weekly or less frequently, depending on ROP Stage and Zone observed in the prior exam⁹. ROP stages^{10,11} and their characteristics are outlined in Table 1.

Expertise in performing indirect ophthalmoscopy, wide-angle digital imaging and image interpretation play a crucial role in ROP management, yet image interpretation is subjective. Examiners employing the latest RetCam imaging disagree 40% of the time as to even the presence or absence of ROP from its earliest stages to preplus and plus disease (i.e., abnormal retinal blood vessel tortuosity and dilation)^{12–14}. There is thus a necessity for imaging methods offering objective, reproducible diagnostic criteria^{11,12,15,16}.

Ophthalmoscopic examination of preterm neonates at risk for ROP has significant limitations beyond subjectivity: Exposure to mydriatic agents, bright light and use of a lid speculum and Flynn scleral depressor to conduct a detailed ophthalmoscopic or RetCam examination of the retina is stressful for the neonate, and not without potential morbidity^{17–21}.

¹Department of Ophthalmology, Columbia University Irving Medical Center, New York, NY, USA. ²Department of Ophthalmology, Columbia University Irving Medical Center, 701 West 168th St., Room 609B, New York, NY 10032, USA. ✉email: rs3072@cumc.columbia.edu

ROP Stage	Characteristics
0	No clear demarcation line between vascularized and non-vascularized retina
1	Demarcation line is visible
2	Demarcation line has developed into a ridge
3	Blood vessels are visible at the ridge
4	Sub-total retinal detachment
5	Total retinal detachment

Table 1. ROP Stages and their characteristics.

Optical coherence tomography (OCT) and OCT-angiography (OCTA) have been explored for examination of the preterm eye. They are advantageous with respect to ophthalmoscopy in not requiring exposure to bright lights or scleral depressors and the exam can be performed via the non-dilated pupil (although dilation is advantageous)^{22–24}. OCT, however, is limited to the posterior pole of the eye and provides only structural information. OCTA offers *en face* mapping of the retinal vasculature, and thus assessment of vessel tortuosity, density, and non-perfused areas (e.g., foveal avascular zone area). OCTA, however, is impeded due to eye motion during imaging (> 3 s)^{25,26}.

Unlike ophthalmoscopy, ultrasound does not require mydriatics and unlike OCT can readily image the posterior structures of the eye even through a closed eyelid. Conventional B-scan, however, has relatively poor resolution compared to optical methods and offers no information on retinal vascular structure or blood flow. Hence, the use of B-scan ultrasound in ROP has been limited, with most reports citing its use for detection of retinal detachment^{27–30}. Jokl et al. evaluated the potential of 10–20 MHz ultrasound B-scan to provide diagnostically significant information, reporting detection of the ridge between vascularized and avascular retina³¹ and development of fibrovascular vitreous membranes portending retinal detachment³².

All of the above techniques image structure rather than function. The central role of VEGF upregulation in ROP, however, suggests that ocular blood flow might be increased in ROP. Doppler ultrasound has thus been used to study ocular blood flow, a functional property, in a number of ROP studies, with variable results. Some reports found no differences between ROP and non-ROP eyes³³ or in Stage 1–2 versus non-ROP³⁴. Others reported significantly increased flow velocities in Stage-2 ROP³⁵.

In the conventional Doppler systems utilized in the above studies, a focused ultrasound beam produced by a linear array is scanned to produce two-dimensional B-scan images. At each image position, the instrument must wait for echo data to be received before moving to the next position, which limits imaging speed to hundreds of B-scans per second. In pulsed Doppler, frequency shifts at specific ranges along the lines of sight are measured in real time to determine flow velocity, but with acoustic intensity exceeding FDA guidelines for ophthalmic imaging³⁶.

Plane wave ultrasound (PWU) is an alternative approach that we utilized in a pilot study of 14 preterm neonates where we found increased arterial and venous flow velocities in Stage 3 ROP³⁷. In PWU³⁸, all the piezoelectric elements of a linear array act together to transmit an unfocused wavefront. A focused image is created using a 'delay-and-sum' algorithm that brings echoes reaching each array element into phase by triangulating the time-of-flight from each image position. A B-scan image is thus formed with each transmit, allowing an imaging rate of over 20,000 B-scans/sec. Combining echo data from a series of angled transmits improves sensitivity and resolution³⁹. By recording scans continuously over a cardiac cycle, Doppler analysis can be performed at any pixel position and systolic and diastolic flow velocities determined in post-processing. Furthermore, because the transmitted wavefront is unfocused, acoustic intensity is significantly less than would occur using a conventionally scanned, focused beam. PWU Doppler can be performed in compliance with ophthalmic regulatory standards, which is not the case in studies performed with conventional pulsed Doppler systems. This is a particularly important consideration in imaging the neonatal eye⁴⁰. A representative PWU Doppler image and spectrograms depicting flow over the cardiac cycle is provided in Fig. 1.

Results

Table 2 provides a breakdown of the study population characteristics. ROP Stage at the time of exams is provided in Table 3.

Of the clinical factors, only birthweight (BW) and GA were found to differ significantly by Stage ($p < 0.001$ by ANOVA). Both factors were significantly different with respect to Stage 0 eyes at Stages 2 and 3 ($p < 0.05$) by post-hoc Dunnett's test.

The within exam standard deviations in the CRA were 12.2, 3.5 and 6.7 mmHg for the PSA, EDV and mean velocity respectively, corresponding to coefficients of variation of 0.28, 0.35 and 0.29. Variability in the CRV and SPCA were comparable.

ANOVA (Table 4) showed significant differences in Doppler flow velocity by Stage in the CRA and CRV. Flow velocities were significantly elevated in Stage 3.

Eleven eyes had preplus disease: 2 at Stage-1, 4 at Stage-2 and 5 at Stage-3. There were only 4 Zone-I (region surrounding the optic nerve head) eyes in the study population. Flow velocities were not significantly altered by presence of preplus or Zone-I disease, although this is uncertain given the small numbers of either preplus or Zone-I.

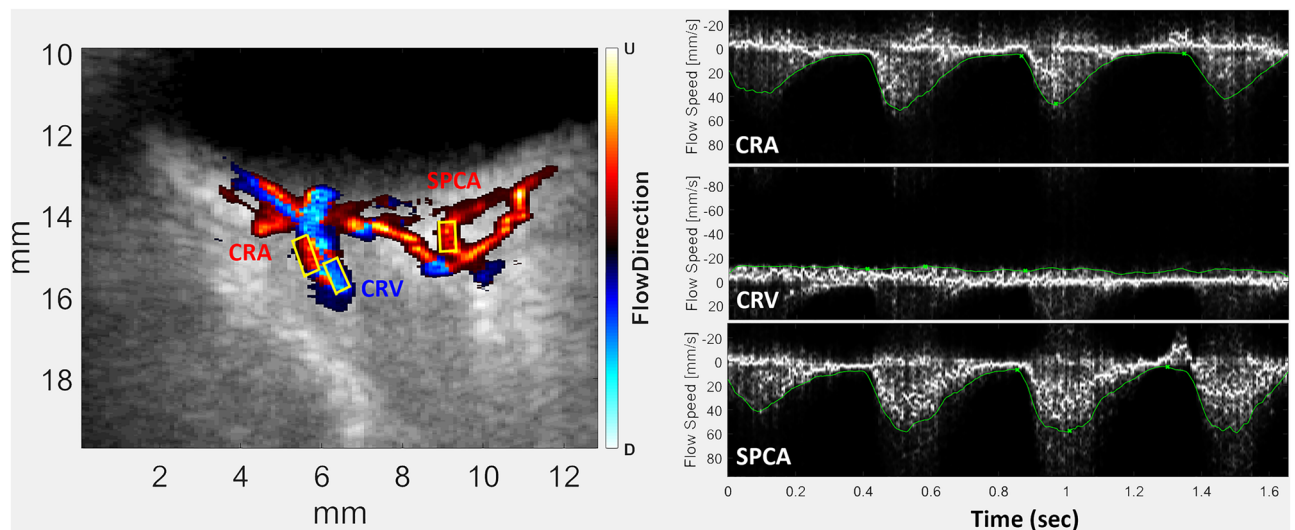


Figure 1. Left: Representative plane-wave color flow Doppler image of neonatal posterior pole. Right: Spectrograms of the CRA, CRV and SPCA.

Factor	Mean \pm SD	Range
Sex	M:76; F:86	
Birthweight (g)	761 \pm 176	410–1370
Systolic blood pressure (mmHg)	78.9 \pm 12.3	54–108
Diastolic blood pressure (mmHg)	48.0 \pm 12.6	24–76
Mean arterial pressure (mmHg)	58.3 \pm 11.4	38.3–85.7
Heart rate (BPM)	143.4 \pm 33.5	57–193
Gestational age (weeks)	26.0 \pm 2.0	20.2–30.2
Post-menstrual age at exam 1 (weeks)	37.2 \pm 3.2	31.5–47.3
Post-menstrual age at exam 2 (weeks)	39.3 \pm 4.1	32.3–50.2

Table 2. Characteristics of neonates.

Stage	Initial exam		Follow up	
	N eyes	%	N eyes	%
0	34	34.0	22	35.5
1	15	15.0	0	0
2	41	41.0	31	50.0
3	10	10.0	9	14.5
Total	100	100	62	100

Table 3. ROP Stage at initial and follow-up exams.

Followup between exams ranged from 14 to 27 days, averaging 21 days. Between initial and followup exams, eight eyes progressed from Stage 1 to Stage 2 and one from Stage 2 to Stage 3. Flow velocity in the CRA and SPCA increased in this group (e.g., by 7.1 ± 15.7 mm/s PSV in the CRA), but given the small number of cases, this was not statistically significant.

Because flow velocities were comparable at Stages 0–2 and increased only at Stage 3, we compared Stage 3 with combined Stages 0–2. ANOVA results comparing flow in Stage 3 versus Stages 0–2 in both the initial exam and follow-up exam are presented in Table 5.

Follow-up exams were performed in approximately 60% of subjects, with dropouts attributable to patient discharge. A noteworthy observation is that in Stage 3 ROP mean flow velocity in the CRA increased on followup by 8.1 ± 20.1 mm/s whereas, the change was only -0.3 ± 9.9 mm/s in Stages 0–2. Although not statistically significant, this increase might be attributable to progression in Stage 3 eyes.

Vessel	Stage	N eyes	PSV (mm/s)	EDV (mm/s)	MV (mm/s)
CRA	0	55	38.2 ± 11.7	9.4 ± 3.6	20.6 ± 6.5
	1	13	42.9 ± 12.6	9.4 ± 3.3	22.2 ± 7.5
	2	70	40.6 ± 13.5	9.0 ± 2.9	21.6 ± 7.3
	3	19	60.5 ± 20.3**	14.0 ± 10.8**	33.6 ± 13.2**
	F		12.9	5.7	13.6
	p		< 0.001	0.001	< 0.001
CRV	0	54	17.7 ± 5.6	12.8 ± 4.8	14.7 ± 5.0
	1	13	17.3 ± 4.5	13.1 ± 4.3	14.4 ± 4.8
	2	71	16.3 ± 5.1	12.2 ± 4.3	13.9 ± 4.5
	3	19	28.3 ± 12.2**	20.5 ± 9.2**	24.1 ± 10.6**
	F		17.6	13.0	16.6
	p		< 0.001	< 0.001	< 0.001
SPCA	0	56	46.3 ± 14.0	13.1 ± 6.2	26.4 ± 9.6
	1	15	50.5 ± 19.6	12.7 ± 4.9	27.3 ± 11.3
	2	72	49.7 ± 13.7	13.4 ± 5.6	28.2 ± 9.3
	3	19	56.7 ± 14.4*	15.9 ± 7.8	32.6 ± 9.5*
	F		2.5	1.2	2.0
	p		0.062	0.328	0.119

Table 4. ANOVA of flow velocity by Stage for each vessel. *Indicates $p \leq .05$ and **indicates $p \leq 0.01$ by post-hoc Dunnett's test with respect to Stage 0.

Vessel	Parameter	All exams		Initial exam		Follow-up exam	
		F	p	F	p	F	p
CRA	PSV	37.2	< 0.001	7.0	0.009	43.0	< 0.001
	EDV	17.0	< 0.001	0.2	0.652	20.6	0.018
	VM	40.4	< 0.001	6.2	0.014	46.1	< 0.001
CRV	PSV	51.6	< 0.001	17.5	< 0.001	40.0	< 0.001
	EDV	38.8	< 0.001	17.8	< 0.001	21.8	0.004
	VM	49.8	< 0.001	18.8	< 0.001	33.3	< 0.001
SPCA	PSV	5.4	0.021	0.5	0.515	10.7	0.002
	EDV	3.3	0.072	0.1	0.831	8.0	0.006
	VM	4.9	0.028	0.2	0.644	12.4	< 0.001

Table 5. One-way ANOVA for Stage 3 versus Stages 0–2 for all exams, initial exam only and follow-up exams only.

Clinical, Doppler and combined clinical + Doppler multivariate classification models are described in Table 6. Their ROC curves are plotted in Fig. 2 and the ROC area under curve for all models are shown in Table 6.

Discussion

The variability of individual measurements was significant, with coefficients of variability of around 30%. This was ameliorated by taking three scans per eye, reducing effective uncertainty of measurement of individual eyes by a factor of $\sqrt{3}$, or 1.73.

We found flow velocities in Stage 1–2 ROP to not differ significantly from Stage 0 eyes, which is consistent with prior studies using pulsed Doppler ultrasound^{34,35}. We also confirmed our preliminary finding of significantly increased flow velocity at Stage 3³⁷.

When comparing blood pressure in Stage 3 versus Stages 0–2, no measures reached statistical significance as univariate parameters, although diastolic blood pressure was borderline elevated ($p = 0.056$, two-tailed) in Stage 3 (53.3 ± 11.6 mmHg versus 47.4 ± 12.6 mmHg in Stages 0–2), and entered into the multivariate stepwise models. We have no hypothesis as to an underlying mechanism, and this remains to be verified in a larger study.

The ROC curves of the multivariate models indicate the tradeoff between sensitivity and specificity that would need to be considered in staging of ophthalmoscopy. We would ideally like a classifier offering 100% sensitivity and specificity for Stage 3 detection, but the best model only achieves perfect sensitivity at 50% specificity, which may represent an unacceptable false-positive rate. At 90% sensitivity, however, the combined model provides ~75% specificity, which may represent a practical tradeoff.

Parameter	Vessel	Standardized coefficient		
		Model 1	Model 2	Model 3
GA		-0.822		-0.417
Diastolic BP		0.624		0.327
MV	CRA		0.488	0.449
PSV	CRV		0.691	0.670
PI	SPCA		0.316	0.311
Correctly classified		64.8%	83.2%	83.9%
Correctly classified validation		64.8%	83.2%	83.9%
AUC		0.760 ± 0.044	0.825 ± 0.060	0.904 ± 0.034
Significance (two-tailed) with respect to Model 1		-	0.417	0.015

Table 6. Discriminant analysis models including only clinical parameters (Model 1), only Doppler parameters (Model 2) and Doppler plus clinical parameters (Model 3). Standardized coefficients represent the weight of each parameter in models.

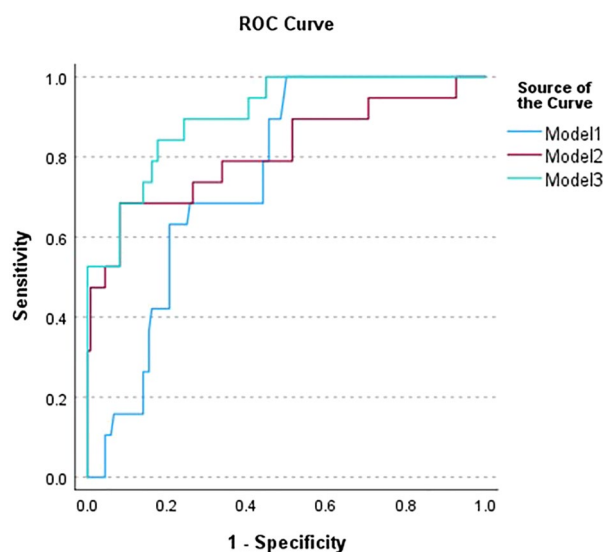


Figure 2. ROC curves for the clinical Model 1, Doppler Model 2, and Doppler plus clinical Model 3.

Since treatment is not normally performed prior to Stage 3, these findings are potentially significant in terms of management: if Stage 3 could be detected by PWU, confirmation by ophthalmoscopy would be prioritized and conversely, if PWU does not indicate Stage 3 ROP, stressful ophthalmoscopic examinations could be performed less frequently.

There are several limitations to this study: Only 11 eyes were preplus and only 4 Zone-I; no patients were imaged pre- and post-treatment by laser or intravitreal anti-VEGF agents; Doppler measurements determined flow velocity, not volumetric flow; ophthalmoscopically determined ROP Stage and presence of preplus disease were treated as ground truth but are themselves subjective.

While the PWU Doppler technology utilized in this study utilized customized software and was implemented on a research ultrasound platform, turnkey PWU systems are now becoming available (albeit not configured for ophthalmology). It is probable that systems suitable for pediatric ophthalmology will in the future offer safe and gentle assessment of ocular blood flow so that these findings could impact ROP management.

In conclusion, PWU could be used to reduce the number of stressful ROP screening dilated ophthalmoscopic exams that babies would have to undergo. PWU could be combined with additional new screening algorithms to implement even further reduction. Possibly the blood flow measurements could contribute to prognostication and refinement of indications for treatment in combination with ophthalmoscopy and/or photography.

Methods

This research followed the tenets of the Declaration of Helsinki and was approved by the Columbia University Institutional Review Board as well as by a separate neonatal intensive care unit (NICU) research ethics and safety committee. Informed consent was obtained from the parents after explanation of the nature, risks, and benefits of the study.

Neonate subjects were inpatients in the New York-Presbyterian/Morgan Stanley Children's Hospital NICU.

Inclusion criteria

Neonates with a birth weight of ≤ 1500 g or a gestational age of ≤ 30 weeks.

Exclusion criteria

Presence of other congenital ophthalmic disease or cardiovascular disease; prior treatment with laser or intravitreal anti-VEGF agents.

A total of 50 low-birthweight, preterm neonates (100 eyes) were examined. 30 had follow-up exams approximately 2 weeks after their initial exam.

ROP Stage, Zone, and presence of plus disease in each eye were determined by an experienced retinal specialist (JDH) by indirect ophthalmoscopic examination as defined by the International Committee for the Classification of Retinopathy of Prematurity while masked to the PWU results⁴¹.

We performed PWU using a Vantage-128 (Verasonics, Inc., Kirkland, WA) research ultrasound system with a Verasonics L22-14vXLF linear array probe. The probe had an 18-MHz center frequency, 128 piezoelectric elements, a 12.8 mm aperture, and an elevation focal length of approximately 18 mm.

Scanning was performed at cribside in the NICU with the assistance of neonatal ophthalmic nurses (LP, OC). Exams were performed after the afternoon feeding, which made exams easier to perform and obviated concern regarding potential diurnal variation. Exams were performed by a single person (RHS) experienced in the performance of clinical ophthalmic ultrasonography. During the exam, the probe was placed in a viral barrier sheath (Sheathes3D; Sheathing Technologies, Inc., Morgan Hill, CA) filled with a cm of water, and coupled to the upper eyelid with GenTeal (Alcon Laboratories, Inc., Fort Worth, TX) gel with minimal pressure. Scans were performed in a horizontal plane encompassing the optic nerve. B-mode color-flow images were displayed in real time. Once the optic nerve and posterior vasculature were satisfactorily displayed, the system was triggered to acquire PWU compound data from six angled transmits over ± 9 degrees. Data were acquired continuously for 1.5 s at 3000 compound scans per second, and the stack of 4500 phase-resolved images stored for post-processing. We acquired three scans of each eye, repeating scans as necessary if degraded by eye or head movement. Examination of both eyes would typically take about 15 min, with much of this taken up by the 45 s wait to store each ~ 9 GB scan.

Acoustic intensity was compliant with FDA guidelines for ophthalmic diagnostic ultrasound standards³⁶.

Doppler analysis was performed as follows: A singular value decomposition filter and a 10 Hz high-pass filter was applied to the data to suppress stationary or slowly moving structures, leaving only blood flow. This information was then used to produce a color flow image from which the CRA, CRV and short posterior ciliary arteries (SPCAs) were identified. We then sampled each vessel to produce spectrograms depicting flow pulsatile flow velocity over the 1.5 s of each scan. From this, after correcting for vessel angle with respect to the acoustic axis, we measured peak systolic velocity (PSV), end diastolic velocity (EDV) and mean velocity (MV), and computed the pulsatile index, $PI = (PSV - EDV)/MV$ and resistive index, $RI = (PSV - EDV)/PSV$.

Statistical analysis was performed using IBM SPSS Version 29 (IBM Corp., Armonk, NY). Variation of Doppler values within eyes by exam was determined. ANOVA, with post-hoc Dunnett's test, was used to compare Doppler parameters between ROP Stages for each vessel. We examined change of flow velocity with change in Stage between initial and followup exams. Because each eye was classified and imaged separately, we treated each eye as a separate case. However, recognizing that eyes of a given subject tend to be correlated, we additionally performed the analysis separately for right and left eyes.

ANOVA was also performed to evaluate the presence of preplus disease and Zone on flow.

Stepwise linear discriminant analysis was used to produce multivariate classification models to distinguish Stage 3 with respect to Stages 0–2. A priori probabilities for group membership were set equal. Classification accuracy was assessed and validated by a leave-one-out procedure. Receiver operator characteristic (ROC) analysis was performed to evaluate the effectiveness of classification functions.

We first produced a stepwise clinical model by entering sex, blood pressure (systolic, diastolic, mean, pulse pressure), GA and BW into the analysis (Model 1). Next, we produced a model using stepwise variable selection of all Doppler parameters (Model 2). Lastly, we produced a stepwise model simultaneously considering both clinical and Doppler parameters (Model 3).

Data availability

The datasets generated and analyzed during the current study are deposited in the Dryad repository: Plane wave Doppler determination of blood flow in retinopathy of prematurity [Dataset]. Dryad. <https://doi.org/10.5061/dryad.612jm649r>.

Received: 15 December 2023; Accepted: 31 March 2024

Published online: 02 April 2024

References

- Kim, S. J. *et al.* Retinopathy of prematurity: A review of risk factors and their clinical significance. *Surv. Ophthalmol.* **63**, 618–637. <https://doi.org/10.1016/j.survophthal.2018.04.002> (2018).
- Bhatnagar, A., Skrehot, H. C., Bhatt, A., Herce, H. & Weng, C. Y. Epidemiology of retinopathy of prematurity in the US from 2003 to 2019. *JAMA Ophthalmol.* **141**, 479–485. <https://doi.org/10.1001/jamaophthalmol.2023.0809> (2023).
- Dai, C. *et al.* Concurrent physiological and pathological angiogenesis in retinopathy of prematurity and emerging therapies. *Int. J. Mol. Sci.* **22**, 809. <https://doi.org/10.3390/ijms22094809> (2021).
- Patz, A., Eastham, A., Higginbotham, D. H. & Kleh, T. Oxygen studies in retrolental fibroplasia. II. The production of the microscopic changes of retrolental fibroplasia in experimental animals. *Am. J. Ophthalmol.* **36**, 1511–1522 (1953).
- Woods, J. & Biswas, S. Retinopathy of prematurity: From oxygen management to molecular manipulation. *Mol. Cell. Pediatr.* **10**, 12. <https://doi.org/10.1186/s40348-023-00163-5> (2023).

6. Chan-Ling, T., Gock, B. & Stone, J. The effect of oxygen on vasoformative cell division. Evidence that “physiological hypoxia” is the stimulus for normal retinal vasculogenesis. *Investig. Ophthalmol. Vis. Sci.* **36**, 1201–1214 (1995).
7. Chan-Ling, T., Gole, G. A., Quinn, G. E., Adamson, S. J. & Darlow, B. A. Pathophysiology, screening and treatment of ROP: A multi-disciplinary perspective. *Prog. Retin Eye Res.* **62**, 77–119. <https://doi.org/10.1016/j.preteyeres.2017.09.002> (2018).
8. Provis, J. M. *et al.* Development of the human retinal vasculature: Cellular relations and VEGF expression. *Exp. Eye Res.* **65**, 555–568. <https://doi.org/10.1006/exer.1997.0365> (1997).
9. Fierson, W. M. Screening examination of premature infants for retinopathy of prematurity. *Pediatrics* **142**, 3061. <https://doi.org/10.1542/peds.2018-3061> (2018).
10. Molinari, A., Weaver, D. & Jalali, S. Classifying retinopathy of prematurity. *Community Eye Health* **30**, 55–56 (2017).
11. Chiang, M. F. *et al.* International classification of retinopathy of prematurity, third edition. *Ophthalmology* **128**, e51–e68. <https://doi.org/10.1016/j.ophtha.2021.05.031> (2021).
12. Campbell, J. P. *et al.* Diagnostic discrepancies in retinopathy of prematurity classification. *Ophthalmology* **123**, 1795–1801. <https://doi.org/10.1016/j.ophtha.2016.04.035> (2016).
13. Campbell, J. P. *et al.* Plus disease in retinopathy of prematurity: A continuous spectrum of vascular abnormality as a basis of diagnostic variability. *Ophthalmology* **123**, 2338–2344. <https://doi.org/10.1016/j.ophtha.2016.07.026> (2016).
14. Chiang, M. F., Jiang, L., Gelman, R., Du, Y. E. & Flynn, J. T. Interexpert agreement of plus disease diagnosis in retinopathy of prematurity. *Arch. Ophthalmol.* **125**, 875–880. <https://doi.org/10.1001/archophth.125.7.875> (2007).
15. Wallace, D. K., Quinn, G. E., Freedman, S. F. & Chiang, M. F. Agreement among pediatric ophthalmologists in diagnosing plus and pre-plus disease in retinopathy of prematurity. *J. AAPOS* **12**, 352–356. <https://doi.org/10.1016/j.jaapos.2007.11.022> (2008).
16. Koreen, S., Lopez, R., Jokl, D. H.-K., Flynn, J. T. & Chiang, M. F. Variation in appearance of severe zone 1 retinopathy of prematurity during wide-angle contact photography. *Arch. Ophthalmol.* **126**, 736–737. <https://doi.org/10.1001/archophth.126.5.736> (2008).
17. Laws, D. E., Morton, C., Weindling, M. & Clark, D. Systemic effects of screening for retinopathy of prematurity. *Br. J. Ophthalmol.* **80**, 425–428. <https://doi.org/10.1136/bjo.80.5.425> (1996).
18. Epley, K. D., Tychsen, L. & Lueder, G. T. The effect of an eyelid speculum on intraocular pressure measurement in children. *Am. J. Ophthalmol.* **134**, 926–927. [https://doi.org/10.1016/s0002-9394\(02\)01793-2](https://doi.org/10.1016/s0002-9394(02)01793-2) (2002).
19. Moral-Pumarega, M. T. *et al.* Pain and stress assessment after retinopathy of prematurity screening examination: Indirect ophthalmoscopy versus digital retinal imaging. *BMC Pediatr.* **12**, 132. <https://doi.org/10.1186/1471-2431-12-132> (2012).
20. Mukherjee, A. N., Watts, P., Al-Madfaei, H., Manoj, B. & Roberts, D. Impact of retinopathy of prematurity screening examination on cardiorespiratory indices: A comparison of indirect ophthalmoscopy and retcam imaging. *Ophthalmology* **113**, 1547–1552. <https://doi.org/10.1016/j.ophtha.2006.03.056> (2006).
21. Dhaliwal, C. A., Wright, E., McIntosh, N., Dhaliwal, K. & Fleck, B. W. Pain in neonates during screening for retinopathy of prematurity using binocular indirect ophthalmoscopy and wide-field digital retinal imaging: A randomised comparison. *Arch. Dis. Child Fetal Neonatal Ed.* **95**, F146–F148. <https://doi.org/10.1136/adc.2009.168971> (2010).
22. Maldonado, R. S. *et al.* Optimizing hand-held spectral domain optical coherence tomography imaging for neonates, infants, and children. *Investig. Ophthalmol. Vis. Sci.* **51**, 2678–2685. <https://doi.org/10.1167/iovs.09-4403> (2010).
23. Mangalesh, S. *et al.* Preterm infant stress during handheld optical coherence tomography vs binocular indirect ophthalmoscopy examination for retinopathy of prematurity. *JAMA Ophthalmol.* **139**, 567–574. <https://doi.org/10.1001/jamaophthalmol.2021.0377> (2021).
24. Mangalesh, S. *et al.* Macular OCT characteristics at 36 weeks’ postmenstrual age in infants examined for retinopathy of prematurity. *Ophthalmol. Retina* **5**, 580–592. <https://doi.org/10.1016/j.oret.2020.09.004> (2021).
25. Zhou, K. *et al.* Quantitative handheld swept-source optical coherence tomography angiography in awake preterm and full-term infants. *Transl. Vis. Sci. Technol.* **9**, 19. <https://doi.org/10.1167/tvst.9.13.19> (2020).
26. Kothari, N. *et al.* Arm-mounted optical coherence tomography angiography in extremely low birth weight neonates with retinopathy of prematurity. *Am. J. Ophthalmol. Case Rep.* **18**, 100624. <https://doi.org/10.1016/j.ajoc.2020.100624> (2020).
27. de Juan, E., Shields, S. & Machemer, R. The role of ultrasound in the management of retinopathy of prematurity. *Ophthalmology* **95**, 884–888. [https://doi.org/10.1016/s0161-6420\(88\)33090-3](https://doi.org/10.1016/s0161-6420(88)33090-3) (1988).
28. Mazzeo, V. & Perri, P. Echographic findings in infants with ROP. *Doc. Ophthalmol.* **74**, 235–244. <https://doi.org/10.1007/bf02482614> (1990).
29. Lee, K. F. *et al.* Ultrasonographic findings in eyes with retinopathy of prematurity in Malaysia. *Med. J. Malays.* **68**, 39–43 (2013).
30. Maidana, E. J. *et al.* Ultrasonographic findings in eyes with retinal detachments secondary to retinopathy of prematurity. *J. Pediatr. Ophthalmol. Strabismus* **44**, 39–42. <https://doi.org/10.3928/01913913-20070101-05> (2007).
31. Jokl, D. H. *et al.* Comparison of ultrasonic and ophthalmoscopic evaluation of retinopathy of prematurity. *J. Pediatr. Ophthalmol. Strabismus* **41**, 345–350 (2004).
32. Jokl, D. H. *et al.* Is there a role for high-frequency ultrasonography in clinical staging of retinopathy of prematurity? *J. Pediatr. Ophthalmol. Strabismus* **43**, 31–35. <https://doi.org/10.3928/01913913-20060101-04> (2006).
33. Holland, D. R. *et al.* Color doppler imaging of the central retinal artery in premature infants undergoing examination for retinopathy of prematurity. *J. AAPOS* **3**, 194–198. [https://doi.org/10.1016/s1091-8531\(99\)70002-9](https://doi.org/10.1016/s1091-8531(99)70002-9) (1999).
34. Ozcan, P. Y. *et al.* Assessment of orbital blood flow velocities in retinopathy of prematurity. *Int. Ophthalmol.* **37**, 795–799. <https://doi.org/10.1007/s10792-016-0333-1> (2017).
35. Hartenstein, S., Müller, B., Metze, B., Czernik, C. & Bührer, C. Blood flow assessed by color Doppler imaging in retinopathy of prematurity. *J. Perinatol.* **35**, 745–747. <https://doi.org/10.1038/jp.2015.45> (2015).
36. Food and Drug Administration. *Marketing Clearance of Diagnostic Ultrasound Systems and Transducers, Guidance for Industry and Food and Drug Administration Staff* (Food and Drug Administration, 2019).
37. Silverman, R. H. *et al.* Ocular blood flow in preterm neonates: A preliminary report. *Transl. Vis. Sci. Technol.* **10**, 22. <https://doi.org/10.1167/tvst.10.2.22> (2021).
38. Tanter, M. & Fink, M. Ultrafast imaging in biomedical ultrasound. *IEEE Trans. Ultrason. Ferroelectr. Freq. Control* **61**, 102–119. <https://doi.org/10.1109/tuffc.2014.6689779> (2014).
39. Montaldo, G., Tanter, M., Bercoff, J., Bence, N. & Fink, M. Coherent plane-wave compounding for very high frame rate ultrasonography and transient elastography. *IEEE Trans. Ultrason. Ferroelectr. Freq. Control* **56**, 489–506. <https://doi.org/10.1109/tuffc.2009.1067> (2009).
40. Urs, R., Ketterling, J. A. & Silverman, R. H. Ultrafast ultrasound imaging of ocular anatomy and blood flow. *Investig. Ophthalmol. Vis. Sci.* **57**, 3810–3816. <https://doi.org/10.1167/iovs.16-19538> (2016).
41. International Committee for the Classification of Retinopathy of Prematurity. The International classification of retinopathy of prematurity revisited. *Arch. Ophthalmol.* **123**, 991–999. <https://doi.org/10.1001/archophth.123.7.991> (2005).

Acknowledgements

The co-authors wish to acknowledge Danny H.-Kauffmann Jokl, MD for both originating this novel, objective method for ROP detection and for being the driving force to see this concept through to its successful conclusion.

Author contributions

RHS: Wrote paper, performed ultrasound exams, performed statistical analysis. RU: Assisted during patient exams, performed all ultrasound post-processing. JDH: Examined neonates by ophthalmoscopy and classified them. OC: Monitored neonate and assisted during exams. Compiled clinical diagnostic information. LP: Monitored neonate and assisted during exams. Compiled clinical diagnostic information.

Funding

Supported by National Institutes of Health Grant P30 EY019007 (Core Facilities for Vision Research), Jonas Philanthropies and an unrestricted grant to the Department of Ophthalmology of Columbia University from Research to Prevent Blindness.

Competing interests

The authors declare no competing interests.

Additional information

Correspondence and requests for materials should be addressed to R.H.S.

Reprints and permissions information is available at www.nature.com/reprints.

Publisher's note Springer Nature remains neutral with regard to jurisdictional claims in published maps and institutional affiliations.



Open Access This article is licensed under a Creative Commons Attribution 4.0 International License, which permits use, sharing, adaptation, distribution and reproduction in any medium or format, as long as you give appropriate credit to the original author(s) and the source, provide a link to the Creative Commons licence, and indicate if changes were made. The images or other third party material in this article are included in the article's Creative Commons licence, unless indicated otherwise in a credit line to the material. If material is not included in the article's Creative Commons licence and your intended use is not permitted by statutory regulation or exceeds the permitted use, you will need to obtain permission directly from the copyright holder. To view a copy of this licence, visit <http://creativecommons.org/licenses/by/4.0/>.

© The Author(s) 2024